

Tom 49(63), Fascicola 1, 2004

Fingerprint recognition using Gabor filters and Wavelet features

Tudosă Ana Maria¹, Costin Mihaela², Barbu Tudor³

Abstract – Amongst the several approaches on fingerprint matching, the most popular continues to be minutiae based. But this technique does not use much of the discriminatory information available in the fingerprints, because local ridge structures cannot be completely characterized by minutiae, further more these methods are slow in comparing fingerprint images containing different number of minutiae. Our method uses a combined structure of Gabor filters and Wavelet features, in order to obtain a well balanced aggregated decision. The recognition system is reinforced in a biometric approach, using in parallel a speaker recognition module. The final decision is obtained by using Dempster - Schafer evidence theory in a hierarchic structure.

Keywords: fingerprint, texture, Fourier transform, Gabor filter, Wavelet, Hausdorff metric, Dempster-Schafer evidence theory.

I. INTRODUCTION

We live in a society where secrets are harder to be kept (locks can be jammed, codes can be broken), therefore issues like security and personal recognition need a solution. Biometrics-based verification, especially fingerprint-based identification becomes the answer to a lot of these problems.

A fingerprint is a pattern believed to be unique across individuals, even across fingers of the same individual, although this has not been proven, and it has one of the highest levels of reliability. The uniqueness of a fingerprint is determined by the overall pattern of ridges and valleys as well as the minutiae points (local ridge anomalies).

Our method uses Gabor filters and Wavelet features. Gabor filters are used to capture both the local and global details in a fingerprint image, in a fixed length vector called *Feature Map*. The result of a Wavelet decomposition of an image on J octaves represents image details in different scales and orientations.

II. IMAGE FILTERING USING GABOR FILTERS

Gabor filters capture local orientation and frequency information. By tuning a Gabor filter to a specific frequency and direction, the local frequency and orientation information can be extracted.

An even symmetric Gabor filter has the following general form:

$$g(x, y, T, \theta) = \exp\left(-\frac{1}{2}\left[\frac{x_\theta^2}{\sigma_x^2} + \frac{y_\theta^2}{\sigma_y^2}\right]\right) \times \cos\left(\frac{2\pi x_\theta}{T}\right) \quad (1)$$

$$x_\theta = x \cos \theta + y \sin \theta \quad (2)$$

$$y_\theta = -x \sin \theta + y \cos \theta \quad (3)$$

where T gives the frequency of the sinusoidal plane wave at an angle θ with the x-axis and σ_x and σ_y are the standard deviations of the Gaussian envelope along the x and y axes respectively.

For extracting the response of the ridge at various orientations of the Gabor filter the parameters T, θ , σ_x and σ_y are set the following values: the frequency T corresponds to the inner-ridge distance in fingerprint images.

For the 300 x 600 (500 dpi) images the average distance is 8 pixels, thus $T = 1/8 = 0.125$. Deciding the values of the standard deviation involves a trade off between noise robustness and precision.

After experimental results we settled on $\sigma_x = \sigma_y = 4$.

We examine the images at 8 different orientations: 0° , 22.5° , 45° , 67.5° , 90° , 135° , 157.5° .

Filtering the fingerprint image with a Gabor filter means convoluting the Fourier transform of the initial image $F(I)$, with the Fourier transform of the filter $F(G_\theta)$, in the frequency domain.

The new image is:

¹ University Alexandru Ioan Cuza

² IIT, Romanian Academy, associated UAIC, Iași,
e-mail: mccostin@iit.tuiasi.ro, cstf2004@yahoo.com

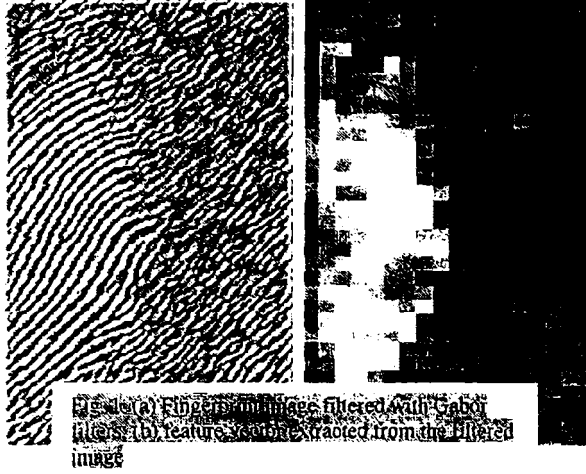
³ Computer Science Institute, IIT, Romanian Academy,
Iași, Dd Carol I, nr. 11A, e-mail: tudbar@iit.tuiasi.ro

$$V_\theta = F^{-1}[F(I)F(G_\theta)] \quad (4)$$

where F^{-1} is the inverse Fourier transform.

A. Constructing the Feature Map

The filtered image can be viewed as a representation scheme but the presence of the local distortions can drastically affect the matching process. more, the local variation in ridge structure together with their global configuration can give a better representation. In order to examine the local variations the image is tessellated and the characteristics of each cell are calculated (Fig.1).



The size of a cell is selected to be twice a ridge size (16 x 16).

Also, when tessellating the image a border of 8 pixels is not used. Considering that the image size is 300 x 600 the feature vector will be 37 x 18 size. The standard deviation corresponds to the energy of the filter response, thus being a useful tool in measuring the ridge orientation in a local neighborhood.

The Feature vector will contain the standard deviation of the pixels in each cell for the 8 filtered images.

B. Fingerprint matching

First the center of the image is computed following an algorithm described in [1]. We improved this algorithm by narrowing the search of the neighborhood in which the center is calculated.

For each template fingerprint in the database we stored 10 *Feature Maps* corresponding to the original image rotated 10°. This will assure that the algorithm is rotation invariant.

The query and the template *Feature Maps* are overlapped on the center point. Each vector is resized to have the same dimension and an Euclidean distance is calculated. A higher distance indicates a poor match. The distance score is then normalized in the [0,100] range, and converted to a similarity score.

For the fingerprints that do not have the same size, the Euclidean distance cannot be used. Therefore, a special nonlinear metric becomes necessary.

For this reason we proposed a nonlinear metric which is able to compare different-sized matrices having a single common dimension, like the fingerprint matrices.

If A and B are two sets having the property $|A| \neq |B|$, the Hausdorff metric [2-4] is defined as the *maximum distance of a set to the nearest point in the other set*. It can be described by the following relation:

$$h(A, B) = \max_{a \in A} \{ \min_{b \in B} \{ dist(a, b) \} \} \quad (5)$$

where h represents the Hausdorff distance between these sets and $dist$ is any metric between their points (for example the Euclidean distance).

In this case we have to compare two matrices instead of two sets of points. Therefore, let us consider $A = (a_{ij})_{n \times m}$ and $B = (b_{ij})_{n \times p}$ the two matrices, with $m \neq p$

Let us introduce two more vectors, $y = (y_i)_{1 \times n}$ and $z = (z_i)_{m \times 1}$, then compute $\|y\|_p = \max_{0 \leq i \leq n} |y_i|$ and

$\|z\|_m = \max_{0 \leq i \leq m} |z_i|$. Using these notations we create a

new nonlinear metric d , having the next form:

$$d(A, B) = \max \left\{ \begin{array}{l} \sup_{\|y\|_p \leq 1} \inf_{\|z\|_m \leq 1} \|By - Az\|_n \\ \sup_{\|z\|_m \leq 1} \inf_{\|y\|_p \leq 1} \|By - Az\|_n \end{array} \right\} \quad (6)$$

The obtained restriction based metric represents the Hausdorff distance between the sets $B(y : \|y\|_p \leq 1)$

and $A(z : \|z\|_m \leq 1)$ in the metric space R^n [3,4].

So, it can be expressed as following:

$$d(A, B) = h(B(y : \|y\|_p \leq 1), A(z : \|z\|_m \leq 1)) \quad (7)$$

It is obviously that the metric d depends on y and z . By eliminating these terms, we have got a new distance. It does not depend on these vectors and it is not a Hausdorff distance anymore. The new obtained Hausdorff-based metric is described as:

$$d(A, B) = \max \left\{ \begin{array}{l} \sup_{1 \leq k \leq p} \inf_{1 \leq j \leq m} \sup_{1 \leq i \leq n} |b_{ik} - a_{ij}| \\ \sup_{1 \leq j \leq m} \inf_{1 \leq k \leq p} \sup_{1 \leq i \leq n} |b_{ik} - a_{ij}| \end{array} \right\} \quad (8)$$

The nonlinear function d , given by (8), verifies the distance properties: positively ($d(A, B) \geq 0$), symmetry ($d(A, B) = d(B, A)$) and triangle inequality ($d(A, B) + d(B, C) \geq d(A, C)$).

From our tests it resulted that it constitutes a satisfactory discriminator between feature vectors [3.4].

We used it also in several speech recognition contexts, for classifying the *DDMFCC* vocal feature vectors [3.4].

Here, the feature vectors are represented by those fingerprints, which can be successfully compared via this Hausdorff based distance.

III. IMAGE FILTERING USING WAVELET FEATURES

Wavelet transforms have important characteristics that make them valuable tools, for many tasks in signal processing. The 2D wavelet decomposition on J octaves of a discrete image represents the image in terms of $3J+1$ sub-images, where each sub-image is a low resolution approximation of the original image containing the image details at different scales and orientations. Wavelet coefficients of large amplitude correspond to vertical high frequencies (horizontal

edges), horizontal high frequencies (vertical edges), and high frequencies in both directions.

The energy of different sub-bands gives information regarding both the ridge spatial frequency as well as the ridge orientation.

Another *Feature Map* is constructed based on the standard deviation of each wavelet sub image. This feature vector has important discriminatory properties for fingerprint images.

A. Fingerprint matching

First we crop the image in an $N \times M$ rectangular region centered in the center point of the fingerprint, then we divide the new image into non-overlapping blocks of $W \times W$ size. For each block we compute the wavelet decomposition on J octaves and calculate its $3J$ wavelet features. The *Feature Map* includes the wavelet features extracted from all $W \times W$ blocks of the central sub-image.

In the second stage of the matching process, the feature map resulted from the Wavelet decomposition is evaluated using a C5 classifier (which is a decision tree constructed on ID3 principles) [5] and a MLP classifier [6].

The results are combined in an aggregation system.

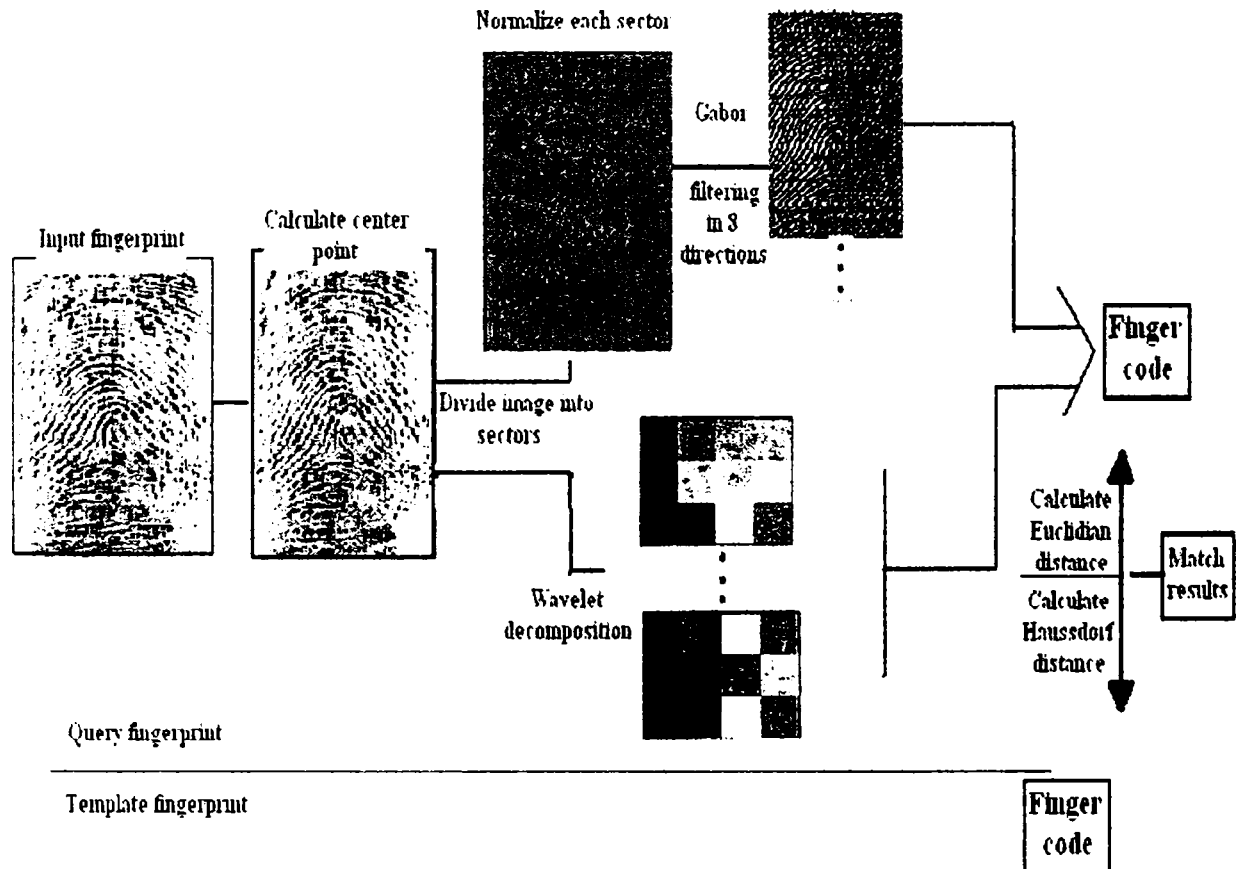


Fig. 2 Flow diagram of our fingerprint identification system

IV. COMBINING THE RESULTS

The results from these two stages, Gabor and Wavelet filtering, are correlated using a decision inferential system based on Dempster-Shafer evidence theory [7], [8]. The different modules play the different specialized "experts". In the aberrant results cases, the conflict has to be managed (re-evaluation on the basis of more criteria or supervised). The importance of each "expert module" is different.

A total mass of belief is calculated for each detected person (from the fingerprint base) and each voice (in the priory registered base) according to the Dempster's rules [DS]. In the belief and plausibility models each time a function (among *mass, m, belief, bel, plausibility, pl* or *communality function, q*) is introduced. The declaration of one of them automatically implies the others, the supplementary symbols being sufficient to know ones are interrelated". Given two belief functions bel_1 and bel_2 induced by two distinct pieces of evidence on the event A, the belief function $bel_{1,2}$ that results from their combination is obtained by Dempster's rules of combination and expressed with communality functions they becomes:

$$q_{12}(A) = q_1(A)q_2(A)$$

In the previous relation, the communality function is a function $q : \Omega \rightarrow [0,1]$, such that, for two events A and B we have:

$$q(A) = \sum_{B \rightarrow A} m(A \vee B)$$

Studying a number of N given fingerprints, a confidence measure corresponding to each of the two applied measures is established.

V. EXPERIMENTAL RESULTS

A database of 140 fingerprint images of size 300x600 including 10 images per finger of 5 individuals has been used in our experiments. The images have been selected from the database based on the fingerprints pattern inside the image, being preferred those where the core point is located close to the center of the image.

Images with poor quality or having the core point too close to the margin of the image have been rejected.

The experiments were performed on a Pentium™ IV, 1800 MHz processor, running Windows XP™. Calculating the center point took ~1.5 seconds, extracting *Feature Map* based on Gabor filters took ~28s, while the time taken to extract the *Feature Map* based on Wavelet decomposition took ~20 s. The time taken to match two *Feature Maps* was ~0:05s, and correlating the results ~ 0:07s.

Table 1

σ	Gabor	Daubechies 10	Our method
0.125	87.1	90.7	95.7
0.142	70.9	85.1	83
0.1	75.1	65.1	80.9

VI. TOWARDS A COMBINED BIOMETRIC SYSTEM

Using a mono modal biometrics an identity verification system has to take a high reliable decision (wished to be less than 0.001% error!), in the context of sensor noise and various limitations of feature extractor and matching, which is a tough, challenging task. Combining multiple biometrics may enhance the performance and accuracy of our personal authentication system. The fingerprint recognition system may be reinforced applying a parallel structure with a voice recognition module [9], [10].

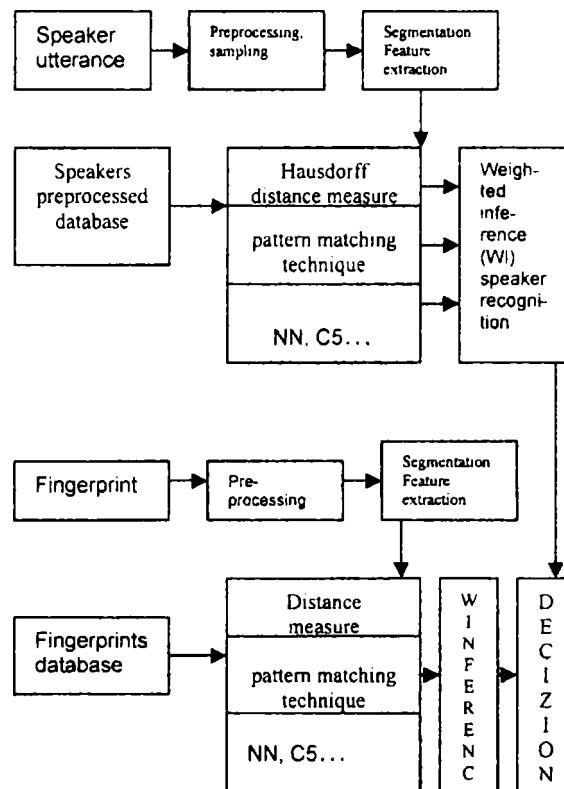


Fig. 3. Biometric recognition - inference modules

Hence, it is possible to establish or to verify the person identity in a double security system in order to have an improved certainty coefficient. This implies comparing more methods in the context of combining the voiceprint and fingerprint recognition system in two different matters: verification and identification.

A rule-based aide decision system gives the final recognition percentage on the person identity.

REFERENCES

- [1] A. Rossa, A. Jain, J. Reismanb, "A hybrid fingerprint matcher", The Journal of Pattern Recognition Society, 2001.
- [2] N. Gregoire, M. Bouillot, "Hausdorff distance between convex polygons", Web project for the course CS 507 *Computational Geometry*, McGill University, 1998.
- [3] T. Barbu, "Discrete Speech Recognition using a Hausdorff-based Metric", Proceedings of the 1st International Conference of E-Business and Telecommunication Networks, ICETE 2004, Aug. 2004, Vol 3, pp.363-368.
- [4] M. Costin, T. Barbu, A. Grichnik, "Tips on Automatic Speaker Recognition, New Decision Tools", CD - ECIT 2004.
- [5] R. Quinlan, CS, 1997, <http://www.ph.th.tudelft.nl/PRInfo/software>
- [6] S. Haykin, *Neural Networks*, MacMillan College Publ. Co., Inc., USA, 1994.
- [7] Ph. Smets, E.H. Mamdan, Didier Dubois, Henri Prade, *Logics for Automated Reasoning*, Academic Press, 1988.
- [8] P. Shenoy, G. Shafer, K. Mellouli, "Propagation of Belief Functions, a Distributed Approach", *Uncertainty in Artificial Intelligence 2*, ed. J.F. Lemmer, L. N. Kanal, Elsevier Science Publisher, pp 325-335, 1988.
- [9] M. Costin, A. Grichnik, M. Zbancioc, "Tips on speaker recognition by autoregressive parameters and connectionist methods", International IEEE Conference SCS, Proc., Vol. 1, pp. 169 – 172, 2003.
- [10] M. Costin, D. Galea, "Decision and Evaluation in Speaker Recognition Connectionist Attempts: New Methods and Trials", to appear on CD Proceedings of SACCS 2004.
- [11] C.J. Lee, S.D. Wang, Kuo-Ping Wu, "Fingerprint Recognition using Principal Gabor Basis Function", Proceedings of 2001 International Symposium on Intelligent Multimedia, Video and Speech Processing, Hong Kong, 2001.
- [12] <http://www.fbi.gov>
- [13] Anil K. Jain, S. Prabhakar, L. Hong, „FingerCode: A Filterbank Fingerprint Representation and matching”, IEEE Transactions on Image Processing, 9 (5) 846-859, 2000
- [14] J.C. Amengual, A. Juan, J.C. Perez, F. Prat, S. Saez, J.M. Vilar, „Real-Time minutiae extraction in fingerprint images”
- [15] N. Ratha, K. Karu, S. Chen, A. Jain, "A Real-time Matching System for Large Fingerprint Databases", (1996), IEEE Transactions on Pattern Analysis and Machine Intelligence, <http://citeseer.ist.psu.edu/cache/papers/cs/1599/ftp.zSzzSzfcp.smsu.edu.zSpubzSzpripzSzrathazSzparni.pdf/ratha96realtime.pdf>
- [16] D. Simon-Zorita, J. Ortega-Garcia, S. Cruz-Llanas, J. Gonzalez-Rodriguez, „Minutiae extraction scheme for fingerprint recognition systems”, <http://ccrma.stanford.edu/~jhw/bioauth/fingerprints/00958099.pdf>
- [17] D. Simon-Zorita, J. Ortega Garcia, S. Cruz Llanas, J. L. Sanchez Bote, J. Glez Rodriguez, "An Improved Image Enhancement Scheme for Fingerprint Minutiae Extraction in Biometric Identification", *Proceedings of the Third Audio and Video-Based Person Authentication*, Halmstad, Sweden, 6-8 June, 2001.
- [18] N. K. Ratha, S. Chen, A. K. Jain, "Adaptive flow orientation based feature extraction in fingerprint images", http://citeseer.ist.psu.edu/cache/papers/cs/1599/ftp.zSzzSzfcp.smsu.edu.zSpubzSzpripzSzrathazSzfeat_ext.pdf/ratha95adaptiv.pdf